Published version available at: https://doi.org/10.1016/j.combustflame.2022.112371

Flame-acoustics interaction for flames propagating from the open to the closed end of a channel: effects of heat losses and the Lewis number

Carmen Jiménez and Vadim N. Kurdyumov

Abstract

In this paper we present a numerical study of the impact of heat losses and the differential diffusion effect on the flame-acoustics interaction, for flames propagating from the open to the closed end of a planar channel. It has been recently demonstrated [1] that for Le=1 symmetric and non-symmetric flames produce different acoustic responses in adiabatic channels. The results of the present study show that the interaction of the flame with the acoustic field is significantly influenced by heat losses and the Lewis number through a change in the shape of the flame: increasing the heat losses tends to make the flames symmetric and low Lewis numbers result in non-symmetric flames.

Keywords:
premixed flames; flame instabilities; thermo-acoustic instabilities;
non-symmetric flames; heat-losses.

1. Introduction

It is well known that the coupling of the flame heat release fluctuations and the acoustic waves traveling in a duct can result in thermo-acoustic instabilities, producing noise, uncontrolled flame behaviour and even structural

damage when the pressure oscillations are large. This phenomenon is especially noticeable when the flame propagates from the open to the closed end of the duct, a configuration where the reflection of acoustic waves at the ends of the channel can be very intense, as shown in experiments in [2–9].

In the numerical modeling of flames propagating in a duct, it has been often assumed that the flame should be symmetrical about the middle of the channel, when modeling planar channels, or about the channel central axis, in channels with circular cross section. This assumption is convenient to reduce computational costs, since the numerical domain can be reduced when the appropriate symmetry boundary conditions are set. However, it has recently been shown that, in addition to the symmetrical flame solution, other types of flames can exist whose shape is not symmetrical [10–19]. These two types of solutions can exist simultaneously, at least as mathematical objects, both in the case of stationary flame propagation (with a constant velocity relative to the channel wall) and in cases where the flame velocity changes with time. The specific shape of the flame that is actually realized, symmetrical or asymmetrical, depends on the values of parameters such as the channel width, the reactants mass flow rate, the wall thermal properties, the thermal expansion rate or the reactants Lewis numbers [19]. An important practical implication is that symmetric and non-symmetric flames present very different flame burning and propagation speeds, with non-symmetric flames being notably faster due to an increased flame surface area. Moreover, when the two solutions exist, in a vast majority of cases, non-symmetric flames are stable while symmetric flames are unstable. It should be noted, however, that despite the possible instability of symmetric flames, their numerical simula-

tion can be easily carried out in a half channel and, thus, their properties can be studied. This symmetry-breaking phenomenon can be linked to hydrodynamic and thermodiffusive instabilities, so that non-symmetric steadily propagating flames appear for $Le < 1$ and even at $Le = 1$ (for a given range of flow rates and channel widths). The existence of non-symmetric flames with oscillatory dynamics was also observed in [11] for $Le > 1$.

Morphological differences between symmetrical and non-symmetrical flames are, of course, reflected in the interaction of the flame with the acoustic field. For $Le = 1$ flames propagating from the open to the closed end of an adiabatic channel the coupling flame-acoustics has been shown to depend on the flame shape. As a consequence, symmetric and non-symmetric flames not only propagate at different speeds but also present different acoustically-driven oscillations [1]. The measured frequency of these oscillations was well approximated in all the studied cases in [1] by the solution of the eigenmode equation for longitudinal acoustic waves in a narrow channel of length L when the flame is considered as a moving passive thin surface separating quiescent gases at the conditions of the fresh gases and the burnt gases. This eigen-frequency is an increasing function of the flame distance to the channel closed end, x/L. However, the flame response to acoustic forcing at these eigen-frequencies, the flame transfer function, was shown to be different for symmetric and non-symmetric flames. In particular, at the frequencies corresponding to the shorter channels studied in [1] (lengths about 800 times the thermal flame thickness δ_T), only symmetric flames had a small but appreciable amplifying response and therefore only symmetric flames presented self-sustained acoustic oscillations, that became more important as L was

increased. For the longer channels, starting at about $L = 1600\,\delta_T$, both non-symmetric and symmetric flames presented large enough amplification. This analysis explained why for some channel lengths only symmetric flames would present acoustic-driven oscillations while for other channel lengths only non-symmetric flames would oscillate, but was only applicable to the case of adiabatic channel walls. Other numerical studies on the two-way coupling between flame and acoustics were presented in [20–22], also with adiabatic walls. In [21, 22], however, the possibility of symmetric and non-symmetric propagating flame solutions was overlooked.

The purpose of the present work is to extend our previous study [1] and include the effects of non-adiabatic walls and differential diffusion on the flame shape and on flame-acoustics coupling. According to the authors, this aspect of the interaction of the flame with the acoustic field has not been considered before. A priori, two effects would be expected when heat losses are increased: on the one side the flame burning rate and therefore the acoustic oscillations should be damped and on the other side symmetric flames should become more stable, as reported in, e.g., [16, 19]. On the other hand, for $Le < 1$ we should expect the flames to become non-symmetric and as a consequence faster for a wider range of conditions. The combined effect of heat losses and $Le < 1$ may then result in damped or enhanced acoustic oscillations and this is studied here using numerical calculations.

In [7, 23–25], where flames in vertical channels were investigated, it was shown that the gravitational acceleration plays also an important role in the acoustic flame instability. However, to limit the scope and extension of the present work, we neglect gravity in the present study, and will study its effect

elsewhere. This research is also limited to the study of planar channels, due to the increased cost involved in the study of three-dimensional configurations. Results of three-dimensional studies will be presented in future work.

The paper is organized as follows: in Section 2 we present the equations governing the problem and the method used for their solution, Section 3 presents results of simulations of symmetric and non-symmetric $Le = 1$ flames in channels with heat losses and Section 4 focuses on the effect of varying the Lewis number. Finally, Section 5 presents conclusions and a summary of the results.

2. Mathematical formulation and numerical solution

Consider a premixed flame propagating in an open-closed planar channel of width D and length L, filled with a fuel/air mixture at initial temperature T_0. The unburned mixture in the region between the moving flame and the closed end of the channel at the left side remains motionless on average, except for the movement of gas particles produced by sound waves (as shown in [1], the oscillating pressure gradient induces a small flux in the fresh gases, switching between positive and negative values opposed in phase to the pressure oscillations). A parabolic-like velocity profile drives the hot combustion products to the exit at the right side of the channel. This non-uniform flow field (and the heat losses to the wall, in case they are present) induces a curvature in the flame, whose magnitude and shape depend on the parameters of the problem. The flame front propagating from the open to the closed end (right to left in the sketch of Fig. 1) can be symmetric or non-symmetric. The exact shape and burning rate of this flame can be determined numerically

by solving the governing equations of the problem.

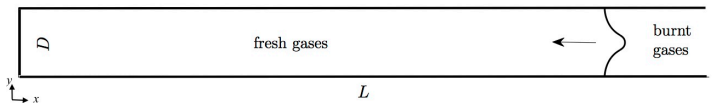

Figure 1: Sketch of the problem

We neglect body forces and radiation heat losses and assume a one-step binary irreversible chemical reaction F + O → P, and a mixture deficient in fuel, so that the oxidant mass fraction remains approximately constant. The resulting 2D conservation equations for mass, momentum, energy and fuel mass fraction are:

$$\frac{\partial \rho}{\partial t} + \frac{\partial \rho u_i}{\partial x_i} = 0 \tag{1}$$

$$\frac{\partial \rho u_i}{\partial t} + \frac{\partial \rho u_i u_j}{\partial x_j} = -\frac{\partial p}{\partial x_i} + \frac{\partial \tau_{ij}}{\partial x_j} \tag{2}$$

$$\frac{\partial \rho e_t}{\partial t} + \frac{\partial \left(\rho e_t + p\right) u_i}{\partial x_i} = \frac{\partial u_i \tau_{ij}}{\partial x_j} - \frac{\partial q_i}{\partial x_i} + Q\,\dot{\omega} \tag{3}$$

$$\frac{\partial \rho Y}{\partial t} + \frac{\partial \rho Y u_i}{\partial x_i} = \frac{\partial}{\partial x_j}\left(\rho\,\mathcal{D}\frac{\partial Y}{\partial x_j}\right) - \dot{\omega}, \tag{4}$$

with $u_i (i = 1, 2)$ the components of the gas velocity, ρ its density, p the pressure, Y the fuel mass fraction and e_t the total (non-chemical) energy, defined as $e_t = \frac{1}{2}u_k u_k + p/\rho\,(\gamma - 1)$, with $\gamma = c_p/c_v$, the ratio of the gas constant-pressure and constant-volume heat capacities, assumed constant, and where the perfect gases equation of state: $p = \rho\mathcal{R}T = \rho(c_p - c_v)T$ is used.

These equations are completed by the definition of the viscous stress tensor, $\tau_{ij} = \mu\left(\partial u_i/\partial x_j + \partial u_j/\partial x_i - \frac{2}{3}\delta_{ij}\partial u_k/\partial x_k\right)$, with μ the mixture dy-

namic viscosity, and the heat flux, $q_i = -\lambda \partial T/\partial x_i$, with $\lambda = \mu c_p/Pr$ the gas thermal conductivity, defined as a function of μ, c_p and a constant Prandtl number Pr. The viscosity and thermal conductivity of the gas mixture are assumed to vary with temperature, as $\mu/\mu_0 = \lambda/\lambda_0 = (T/T_0)^{0.7}$. The fuel mass diffusivity $\mathcal{D}$ is $\mathcal{D} = \mathcal{D}_T/Le$, with $\mathcal{D}_T = \lambda/(\rho c_p)$ the thermal diffusivity and Le a constant Lewis number, so that $\mathcal{D}$ and $\mathcal{D}_T$ depend on temperature as $\rho\mathcal{D}/\rho_0\mathcal{D}_0 = \rho\mathcal{D}_T/\rho_0\mathcal{D}_{T0} = (T/T_0)^{0.7}$. The subscript 0 stands for variables measured in the fresh gas mixture.

As mentioned above, the mixture is assumed to be deficient in fuel, so that the oxidizer mass fraction is considered constant and the fuel mass consumption rate per unit volume and time is modelled via an Arrhenius model as:

$$\dot{\omega} = \mathcal{B}\, \rho^2\, Y\, \exp(-\mathcal{E}/\mathcal{R}T), \tag{5}$$

with $\mathcal{E}$ the activation energy and $\mathcal{B}$ a pre-exponential factor, where Y is the deficient mass fraction. (This corresponds to a very lean mixture, an identical formulation would be obtained if we assumed a very rich mixture and constant fuel mass fraction. In that case Y would represent the oxidizer mass fraction). We introduce the usual Zel'dovich number and thermal expansion parameters: $\beta = \mathcal{E}\,(T_a - T_0)\,/\,(\mathcal{R}\,T_a^2)$ and $q = T_a/T_0$, the standard parameters characterizing Arrhenius models, with T_a the adiabatic flame temperature. The heat produced per unit volume and time, $Q\,\dot{\omega}$, is given by the factor $Q = (T_a - T_0)c_p/Y_0 = (q-1)T_0 c_p/Y_0$. The power $n = 2$ for the density dependence of the reaction rate in Eq. 5 was chosen here as the most representative for combustion. Even if there is a certain controversy on whether it should be $n = 1$ or $n = 2$, we showed in [1] that choosing

$n = 1$ or $n = 2$ only leads to quantitative differences in the flame response to acoustics.

We solve a dimensionless version of Eqs. 1-4, using as characteristic parameters: $\delta_T = \mathcal{D}_{T0}/S_L$, the thermal flame thickness of the planar flame, with S_L the adiabatic planar flame speed, a time scale δ_T/c_0 (with c_0 the speed of sound in the fresh gases, $c_0 = \sqrt{\gamma p_0/\rho_0}$), and the fresh gases reference state given by ρ_0, T_0, μ_0, Y_{F0} and c_p. The only free parameters in the dimensionless equations are: Le, Pr, q, β, γ, the Damköhler number, Da, related to the pre-exponential factor $\mathcal{B}$ as $Da = \mathcal{B}\rho_0\,\delta_T/c_0$, and an acoustic Reynolds number $Re_{\rm ac} = \delta_T\, c_0\, \rho_0/\mu_0$. It should be noted that the choice of a characteristic length equal to the thermal thickness, $\delta_T = \mathcal{D}_{T0}/S_L$, based on the value of the thermal diffusion coefficient estimated for the cold mixture, results in a larger than unity "real flame width", since the value of the thermal diffusion coefficient near the flame is noticeably larger than $\mathcal{D}_{T0}$.

Here we fix a set of parameters: $Pr = 0.7$, $q = 8$, $\beta = 10$, $\gamma = 1.4$ and $Re_{\rm ac} = 476.19$ (the same values used in [1]), and vary the Lewis number Le and the wall thermal properties, as explained later. The Damköhler number Da was chosen to vary with Le, so that for all the flames in this work the planar flame speed S_L takes the same value $S_L = 3 \cdot 10^{-3}\, c_0$. These values of the parameters correspond, for example, to a lean hydrogen-air flame at standard conditions.

2.1. Boundary conditions

Boundary conditions at the walls represent the solid-gas interaction. In this work we will not model the temperature distribution inside the wall along the channel. Instead, we assume a small wall thickness h_w, $h_w/D << 1$,

so that the temperature distribution within the solid wall can be taken as linear between the gas temperature and the external wall temperature, which we take equal the fresh gases temperature, T_0.

We can then write the temperature boundary conditions for the bottom and top walls as done in [12] or [16]:

$$\left.\frac{\partial T}{\partial y}\right|_{y=0} = \frac{\lambda_w}{\lambda h_w}\left(T_{y=0} - T_0\right), \quad \left.\frac{\partial T}{\partial y}\right|_{y=D} = \frac{\lambda_w}{\lambda h_w}\left(T_0 - T_{y=D}\right), \tag{6}$$

where λ and λ_w are the gas and wall thermal conductivities, respectively. The boundary condition for the left wall is set as adiabatic assuming, for example, a large sidewall thickness. These conditions are supplemented by no-slip, no-flux conditions for the velocity and the fuel mass fraction at the walls:

$$u_i|_{y=0} = u_i|_{y=D} = 0, \qquad \left.\frac{\partial Y}{\partial y}\right|_{y=0} = \left.\frac{\partial Y}{\partial y}\right|_{y=D} = 0. \tag{7}$$

The parameter $\lambda_w/(\lambda h_w)$ in Eq. 6 controls the heat transfer between the gas and the solid and depends on the wall thermal conductivity and thickness, which are constants, and on the gas thermal conductivity, λ, which varies with temperature. We will use, as in [16], a reference non-dimensional heat transfer parameter given by the value of the heat transfer parameter at the fresh gases scaled with the flame thickness δ_T:

$$b = \frac{\lambda_w}{\lambda_0}\frac{\delta_T}{h_w}, \tag{8}$$

with λ_0 the thermal conductivity of the unburned gas mixture. A value $b = 0$ corresponds to an adiabatic wall and the limit $b \to \infty$ represents an isothermal wall.

Setting the boundary conditions for the pressure at the open end of the channel is controversial and different options have been used in numerical

studies. In this study, we set a pressure node with constant pressure equal to ambient pressure ($p = p_a$) at the open channel end, representing an outlet open to the atmosphere, as in [1]. Note that this constant pressure boundary condition implies reflection of sound waves at the open end [26, 27]. As a consequence, in addition to the acoustic mode between the flame front and the closed-end wall, the acoustic mode between the flame front and the open end also affects the flame-acoustics interaction, as was the case in [1]. This is different to the flame-acoustics interaction in [21, 22], where non-reflecting boundary conditions were applied at the channel exit so that the flame-acoustics interaction happened only due to the acoustic mode between the flame front and the closed end wall. This constant pressure boundary condition for an open tube has been used in several numerical studies concerning acoustic flame instabilities [28–30].

The NSCBC methodology [26] is used to implement the boundary conditions. In particular the constant-pressure outlet condition is implemented as a subsonic reflecting outflow (see paragraph 9.4.5 in [27]). In some cases with very strong acoustic oscillations, the flow direction in the burnt gases may be occassionally inverted, so that the outlet becomes an inlet. In this case, additional zero gradient conditions for the fuel mass fraction and temperature at the outlet are used.

2.2. Numerical method

We use the compressible solver NTMIX3D, a parallel solver designed for the direct numerical simulation of flames and turbulent reacting flows described in [31], using 6th-order finite differences and 3d-order Runge-Kutta time integration.

The computational domain is a $D \times L$ rectangle, discretized on a uniform Cartesian grid with 100×2000 cells for a channel with $D = 40\ \delta_T$ and $L = 800\ \delta_T$. The same numerical method used in this study was validated in [1]. Details on resolution tests, comparing results in a grid with twice and four times the resolution can be found in the Appendix of [1]. The order of convergence is estimated to be ≈ 1.15. In the present calculations, for some particular cases a grid with a finer resolution was adopted; this will be discussed in the text as these cases are presented.

The question of the adequate resolution needed for flame simulations can be controversial. It is generally accepted that a sufficiently small grid for a planar flame is obtained with about ten points inside the flame thickness δ_L, defined as: $\delta_L = (T_a - T_0) \,/\, \frac{dT}{dx}\big|_{max}$ [27]. For the present planar flame, in particular, we have $\delta_L \approx 6\delta_T$, and a grid about 15 times smaller than δ_L. Of course these are only order of magnitude estimations. Moreover the adequacy of the grid size depends also on the adopted numerical method.

Again replicating the calculations in [1], the simulations are initialized using a planar flame solution near the open end, to avoid the small time steps related to flame ignition. This is done here by computing a steady freely propagating planar flame with the same code and models and using this solution as initial condition for all the calculations. The initial flame is located so that the peak heat release is at a distance $70\ \delta_T$ from the open end. Anticipating the possible existence of symmetric and non-symmetric solutions, two kinds of simulations are implemented:

1. Full-domain simulations, starting from a non-symmetric perturbation

of the planar flame with the shape of a hot spot centered at x_c, y_c:

$$T(x,y) = T_p(x,y)\left[1 + 6\exp\left(-\left((x-x_c)^2 + (y-y_c)^2\right)/2R^2\right)\right], \quad (9)$$

where $T_p(x,y)$ is the unperturbed initial planar flame temperature field and typically $R = \delta_T$, $x_c = L - 80\,\delta_T$, $y_c = 3D/4$;

2. Half-domain simulations, with a computational domain limited to the range $0 < y < D/2$, and with symmetric boundary conditions imposed along the central channel axis $y = D/2$.

The simulations in the full domain reproduce (after an initial transient) the stable flame solution, whether it is symmetric or non-symmetric. The half-domain simulations are used to obtain the symmetric solution for comparison, even in the cases when it is unstable.

Note that when carrying out numerical simulations (or experiments), the following fact should be taken into account. If symmetric (or very near symmetric) initial conditions are chosen but the stable configuration is non-symmetrical, the time for the development of this solution depends on the degree of asymmetry of the initial conditions and the accuracy of the used numerical code. When studying the dynamics of a flame in channels of finite length, this transition time may easily exceed the total travelling time of the flame from the beginning to the end of the channel. In the case of an experiment, the establishment of symmetric conditions (for example at ignition) is even more problematic. For this reason, the transition time from (almost) symmetric initial conditions to a non-symmetric flame shape cannot be a well-defined flame property.

When analysing the results, one of the main characteristics of the dy-

namics is the pressure field, in particular its value at the closed end of the channel, that we denote in this paper p_w. We measure also the flame burning rate or fuel consumption speed (scaled with S_L) defined by the integral:

$$S_c/S_L = \frac{1}{\rho_0 Y_0 \, D \, S_L} \int_0^D \int_0^L \dot{\omega} \, dxdy. \tag{10}$$

The derivation of this property is not new (see, e.g. [27]) and it is given in the Appendix for completeness. It should be mentioned that for adiabatic channels S_c can be associated to a flame propagation speed, when the flame propagates at a constant speed. It must also be said that the numerical value of this integral losses its physical meaning when the flame is located near the right (open) or left (closed) channel ends (see Appendix).

3. Symmetric and non-symmetric $Le = 1$ flames in a channel with wall heat losses

In [1] we showed that for $Le = 1$ flames in adiabatic channels the critical channel width from and above which symmetric flames become unstable and non-symmetric flames appear was $D \approx 17\delta_T$ (for the studied flame parameter values). Moreover, we showed in [1] that there was a critical channel width and length for which self-sustained flame oscillations appear as a result of flame-sound interaction; these critical channel dimensions were estimated to be about $D = 40\delta_T$ and $L = 800\delta_T$.

In this section we present results of simulations for $Le = 1$ flames propagating in a non-adiabatic channel of width and length $D = 40\delta_T$ and $L = 2400\delta_T$. These channel dimensions were chosen so that both symmetric and non-symmetric flames would present self-sustained acoustically-induced

oscillations in the adiabatic channel according to [1]. We compare results of full-domain and imposed-symmetry calculations to demonstrate that when the two kind of solutions may mathematically exist, the non-symmetric flame is the stable solution, as shown before in [1, 19] in cases where the acoustics or the heat losses were neglected.

The simulations were done on Cartesian grids with 100×6000 cells (or 50×6000 cells for the half-domain cases), except for the full-domain, $b = 0.01$ case, for which the flames were more corrugated and stretched and a finer mesh with 150×9000 cells was needed.

Full domain simulations results show that for adiabatic walls or small heat losses the flame becomes non-symmetric, while for large heat losses the flame adopts a symmetric shape. This can be seen in Fig. 2 left, where the flame is non-symmetric for the adiabatic ($b = 0$) and moderate heat transfer ($b = 0.01$) cases, becomes almost planar for $b = 0.02$, and then symmetric with a mushroom shape for larger heat losses. This confirms that the existence of stable symmetric flames is favored by heat losses as reported before in [16, 19].

The flame consumption speed, S_c, and the pressure measured at the closed-end wall, p_w, for the same full-domain calculations are presented in Fig. 3 left. These variables show the coupled flame and pressure oscillations. Starting from the initially planar flame, for which the consumption speed is $S_c = S_L$, the flames acquire curved shapes as they propagate along the channel and accelerate, then they start oscillating. These oscillations can be measured as oscillations in the consumption speed S_c or in the pressure p_w in Fig. 3. The non-symmetric flames in the full domain with small heat losses

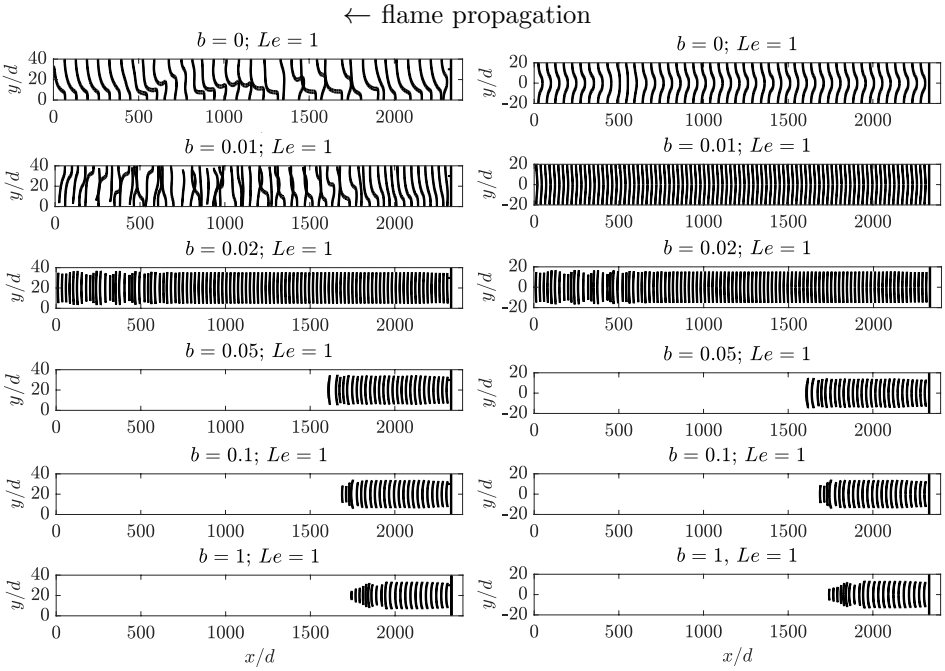

Figure 2: Reaction rate isolines corresponding to $\omega\delta_T/(\rho_0 c_0) = 1$, at time steps $\Delta t = 0.0125L/S_L$, illustrating the propagation of a $Le = 1$ flame in channels with $D = 40\delta_T$, $L = 2400\delta_T$ and varying b, in full-domain (left) and half-domain (right) computations. The initial planar flame is located near the right end of the channel and propagates to the left.

(cases $b = 0, 0.01$ in Fig. 3 left) present larger mean flame speeds and larger amplitude oscillations. Because they are faster, they reach the end wall in shorter times. For larger heat losses ($b > 0.02$) the flames extinguish before reaching the end wall.

In the adiabatic case the flame curvature results in an average flame consumption speed larger than the laminar flame speed (about $2.2S_L$), with oscillations of amplitude of the order of S_L. For increasing values of the

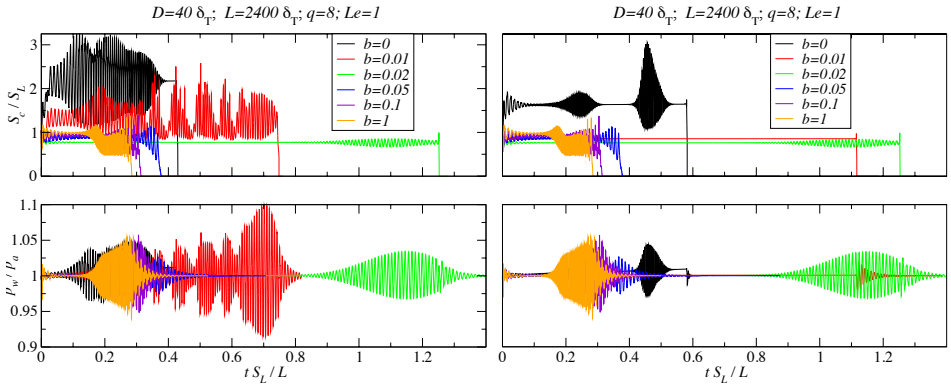

Figure 3: The time evolution of the dimensionless flame consumption speed S_c/S_L and the dimensionless pressure at the end wall p_w/p_a in channels with $D = 40\delta_T$, $L = 2400\delta_T$ and varying b, in full-domain (left) and half-domain (right) computations.

heat losses S_c decreases, reaching a value below S_L for the nearly planar flame ($b = 0.02$). As heat losses are further increased the flame acquires again a curvature and the flame consumption speed increases moderately, to values close to the laminar flame speed S_L. For the non-symmetric flame of the $b = 0.01$ case, pressure oscillations can be relatively important, with a maximum pressure amplitude of up to $10\%p_a$. It is interesting to remark that even if this flame is slowlier than the adiabatic flame, the pressure oscillations, which depend on the flame shape, can be stronger than those found in the adiabatic case.

Oscillations become almost negligeable for the quasi-planar flame with $b = 0.02$, with only appreciable oscillations near the end of the channel, where the flame has acquired a little curvature. This confirms again that the flame-acoustics coupling is dependent on the flame shape and that some flame curvature is necessary for this coupling to occur. Indeed, as shown in [32, 33],

for planar flames the only effect of pressure oscillations on the flame happens via the reaction rate response, which is much less intense that the flame response studied here. Finally, for large values of the heat losses coefficient ($b \geq 0.05$), the flame adopts a symmetric mushroom shape and oscillations appear early in the channel propagation, but flames are extinguished by heat losses before these oscillations become more important.

The effects of heat losses observed here are qualitatively similar to those reported in the experiments in [9] for moderately weak flames ($15-20$ cm/s) propagating in a narrow cylindrical tube ($\varnothing = 8$ mm). In particular, the experiments show that for flames with $S_L = 20$ cm/s heat loss effects are moderate and a rapidly fluctuating flame can propagate to the end of the tube showing large pressure fluctuations, which in [9] are related to the secondary acoustic instability (this corresponds to Figs. 4 c and Fig. 6 in [9]). The pressure trace for this regime is very similar to that found here for small heat losses (case $b = 0.01$ in Fig. 3 left): large oscillations in pressure growing in amplitude along the propagation, that reach peaks of 4kPa in the experiments and 10kPa here. For weaker flames, the experiments show that heat losses are more important. In the case of $S_L = 15$ cm/s, corresponding to Fig. 4 b in [9], the curved flame becomes first nearly planar, with moderately large pressure amplitude oscillations. At some point in the oscillations the flame reaches a maximum flame area and then extinction happens after a strong acoustic oscillation. This is explained in [9] as a possible effect of the large stretch induced in the flame as the oscillations become large and the flame area increases; this stretch would then contribute to extinction. A similar behaviour is observed in the present numerical simulations for the

cases with large heat losses ($b \geq 0.05$ in Fig. 3 left): an increase in the flame consumption speed (and in the flame area) driven by oscillations is detected preceding flame extinction for these cases. As explained in [9], it is a priori possible that steady flames could propagate in the tube in these cases, while vibrating flames with a large area and stretch would be more affected by heat loss and would extinguish. This is an interesting effect that could be confirmed in future work by comparing the present flame simulation results to low-Mach number simulations where acoustic oscillations are neglected.

The right column plots in Figs. 2 and 3 correspond to half-domain simulation results for the same parameters ($Le = 1$, $D = 40\delta_T$ and $L = 2400\delta_T$). Figure 2 right shows that the forced symmetry condition results in a symmetric tulip shape for small heat losses ($b = 0, 0.01$), that become mushroom-shaped for large values of b. The simulations with $b \geq 0.02$ show flames identical to those obtained in the full domain. For these cases the symmetric solution is stable, while for $b = 0$ and $b = 0.01$ it is clearly unstable: if the forced symmetry condition is removed the flame becomes non-symmetric.

For imposed-symmetry calculations, oscillations in the consumption speed and the pressure at the end wall (Fig. 3 right) are small in all cases. Note that in [1] it was shown that the flame response to acoustic pressure oscillations, the flame transfer function, depends on the flame shape, displaying a different frequency dependence for symmetric and non-symmetric flames. Apparently, for the present flame and channel size parameters, the response of non-symmetric flames to the eigen acoustic modes of the channel is more intense at frequencies corresponding to flame positions near the middle of the channel, while symmetric flames present a more intense response at the

higher frequencies near the end wall.

4. Effect of the Lewis number

It is well known that when the Lewis number is less than one, the flame propagating in an unbounded space can acquire a cellular structure. The cellular structure is also possible when the flame propagates in a channel from an open to a closed end, when the gas ahead of the flame is at rest.

In this section we compare results for flames with different Le numbers and varying b propagating in a $D = 40\delta_T$, $L = 800\delta_T$ channel. This is the minimum channel size for which self-sustained acoustic oscillations appear for $Le = 1$ flames in adiabatic channels in the present configuration, according to [1].

All the results below correspond to full-domain unsteady simulations and were done on Cartesian grids with 100×2000 cells, except for certain cases where a finer mesh was needed. This was the case of $Le = 0.3$ flames with $b = 0.01$ and 0.02 (for these cases a 150×3000 grid was needed), and $Le = 0.7$ flames with $b = 0.05$ and $Le = 0.3$ flames with $b = 0$ (cases for which a 200×4000 grid was needed). In these cases very convoluted symmetric flames with large surfaces appear, requiring a finer resolution.

Figure 4 displays the flame consumption speed and pressure at the end wall together with reaction rate isolines representing the flame propagation for $Le = 1$ and different values of the heat transfer coefficient b. Results are similar to those of the previous section: the flames are non-symmetric for low heat losses, become almost planar as heat losses increase, and then symmetric with a mushroom shape for larger heat losses. However, contrary to what

was observed in the longer channel of Fig. 2, for this case with $L = 800\delta_T$, oscillations are negligeable for non-symmetric flames while they can become relatively important (up to 5% of p_a) for the symmetric mushroom-shaped flames (cases with $b \geq 0.05$). This agrees with the results in [1] for adiabatic channels: for $Le = 1$ flames in $D = 40\delta_T$, $L = 800\delta_T$ channels only symmetric solutions present acoustic-driven oscillations.

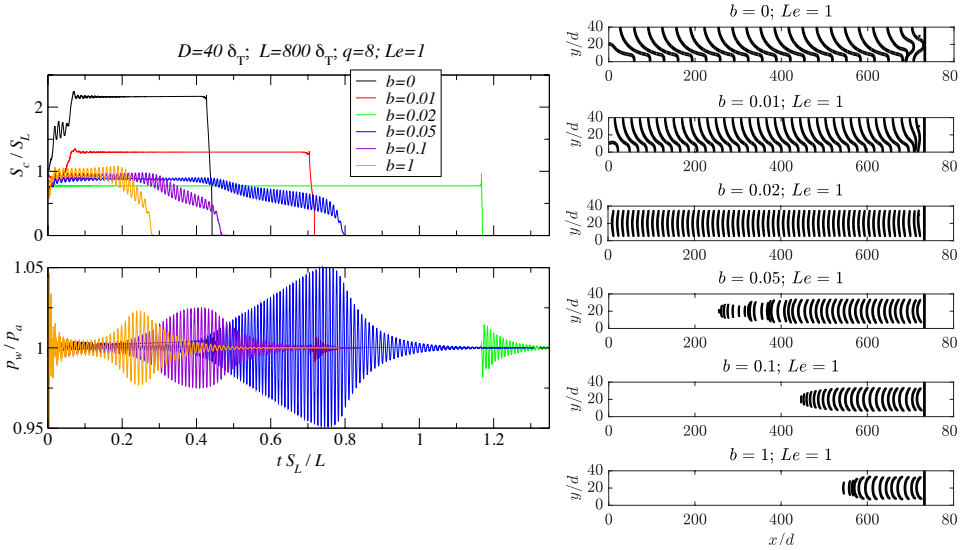

Figure 4: The flame consumption speed, the pressure at the end wall (left) and reaction rate isolines $\omega\delta_T/(\rho_0 c_0) = 1$ (right) for $Le = 1$ and several values of b. Isolines are separated by time intervals $\Delta t = 0.01875L/S_L$.

When the Lewis number is reduced, the flame shape is modified and, accordingly, the response to acoustic oscillations changes as well. It is important to remark that when the Le number is changed the rest of parameters are kept constant, except for Da, which is changed so that the planar flame speed value, S_L, is also maintained constant.

For the $Le = 0.7$ cases, presented in Fig. 5, the flame in the adiabatic channel is non-symmetric, but with a different shape, more corrugated than in the $Le = 1$ case and displaying two cells. Because of this change in shape, the flame burning rate and the pressure oscillations are appreciably larger than in the $Le = 1$ case of Fig. 4. As the heat losses coefficient is increased, the flame shape becomes closer to planar, and oscillations disappear. For even larger heat lossses ($b = 0.05$) we find symmetric flames oscillating between tulip and mushroom shapes, with large oscillations in the flame consumption speed and in the measured pressure, which can become as large as $14S_L$ and $50\%p_a$, respectively. In this case, the flame adopts a very convoluted symmetric shape at the end of the propagation, similar to the violent folding reported in [22]. Note that in [1], where only adiabatic channels were considered, this kind of flame was only obtained in unphysical half-channel simulations, where symmetry was forced.

For larger values of the heat transfer coefficient $b \geq 0.1$, the flame recovers a behaviour close to that of the $Le = 1$ flame, extinguishing before reaching the mid-channel. Apparently, these flames extinguish before reaching the position in the channel corresponding to the more resonant frequencies which, according to the results for $b = 0.05$, should be located at the second half of the channel in this case.

With a further decrease in the Lewis number, the cellular nature of the flame manifests itself in greater force. Figure 6 presents the results of simulations for flames with $Le = 0.3$. For $Le = 0.3$ the flame shape changes drastically, and so do the propagation and oscillation characteristics. In the adiabatic and lower heat losses cases ($b = 0, 0.01$ and 0.02), we observe sym-

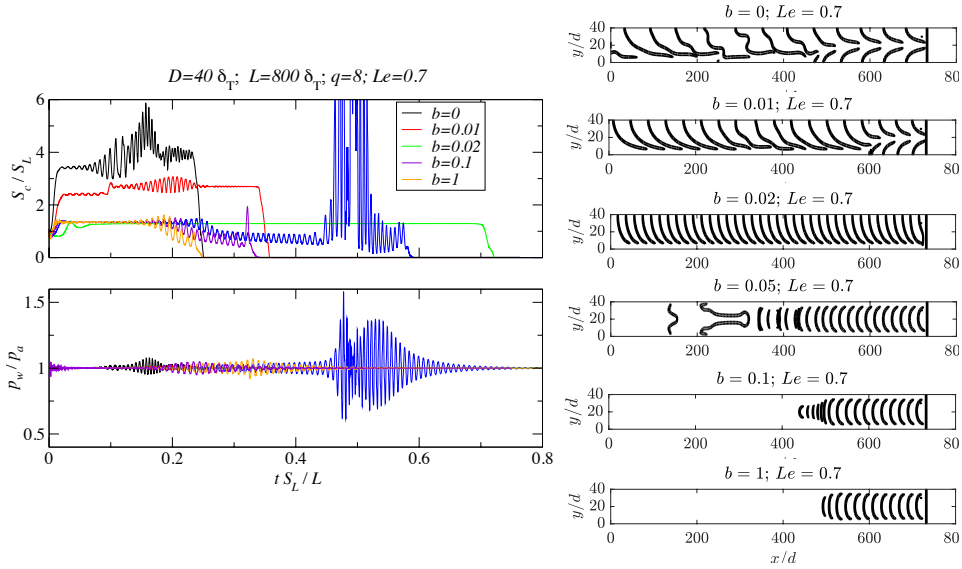

Figure 5: The flame consumption speed, the pressure at the end wall (left) and reaction rate isolines $\omega\delta_T/(\rho_0 c_0) = 1$ (right) for $Le = 0.7$ and several values of b. Isolines are separated by time intervals $\Delta t = 0.01875 L/S_L$.

metric flames which become non-symmetric along the propagation. Both the symmetric and the non-symmetric flames are very convoluted for this low value of Le, and as such, present a large surface and large burning rates, of the order of 10 times S_L. This large flame length and burning speed require a finer mesh in order to adequately solve the flame. Oscillations in the flame speed and pressure are also very large, of the order of 30 S_L and 50% p_a, respectively. These large surface and speed require a finer mesh for adequate resolution. These fast flames reach very quickly the end wall: as can be seen in Fig.6 left, the flames with $b \leq 0.02$ reach the end wall at times $t < 0.1 L/S_L$, that is, they propagate on average ten times faster than the planar flame. This can be compared to the case $Le = 1$ in Fig. 4, for

which the total propagation times were on average of the order of $0.5L/S_L$ and could be as long as $1.2L/S_L$ for the almost planar flame with $S_c < S_L$.

Finally, it is remarkable that for large values of the heat losses (large b), the flames adopt very large curvatures, even breaking into smaller round-shaped cells. This shape confers robustness to the flames, so that even for very large heat losses coefficients these flames can survive and propagate to the end of the channel. This kind of flames resemble those described in [34] in simulations of ultra-lean H_2 flames with radiation heat losses and in [35] in simulations of low Lewis number flames in a Hele-Shaw chamber with large heat losses. Here we report that these flames, in addition to a large burning rate with large resistance to extinction by heat losses, may be linked to large pressure oscillations, as seen for $b = 0.1$ and $b = 1$ in Fig. 6. This is an issue that should be taken into account in the design of lean hydrogen combustion systems, for example, as it affects both the safety under fuel leakages and the stability of the flames in enclosed devices.

5. Conclusions

The main goal of this work is to demonstrate the importance of taking into account the possibility of losing the symmetry of the flame and the influence of this phenomenon not only on the speed of propagation of the flame along the channel, but also on its impact on the interaction of the flame with the acoustic field.

We studied numerically flames propagating from the open to the closed end of a planar channel where reactants are initially at rest. In this channel configuration, the manifestation of the interaction between the flame and

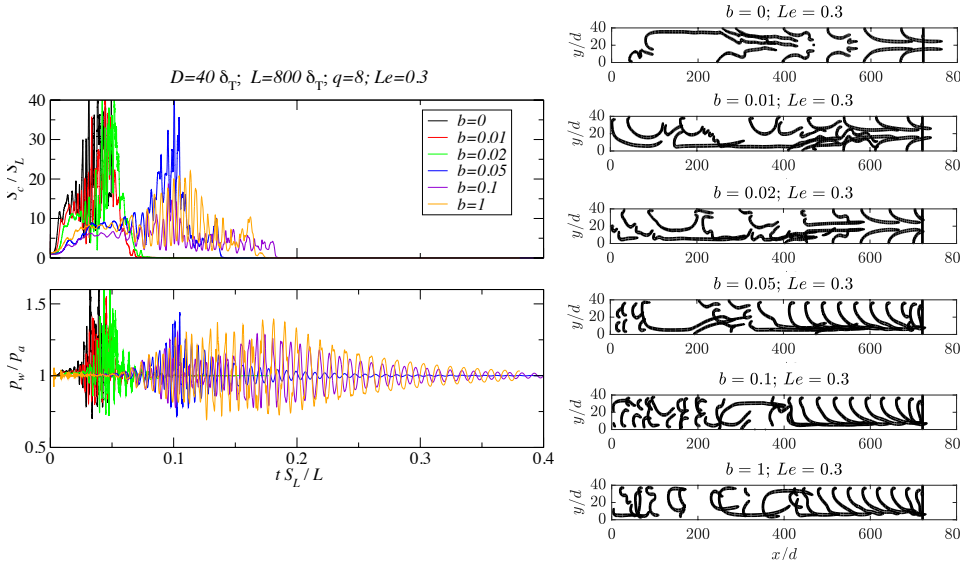

Figure 6: The flame consumption speed, the pressure at the end wall (left) and reaction rate isolines $\omega\delta_T/(\rho_0 c_0) = 1$ (right) for $Le = 0.3$ and several values of b. Isolines are separated by time intervals $\Delta t = 0.0075L/S_L$.

the acoustic field is most pronounced. The study focuses on the effect of the channel wall thermal properties and the Lewis number on the flame shape and, as a consequence, on the flame-acoustics interaction. This is an extension of a previous study in which only adabiatic channels and flames with $Le = 1$ were considered [1].

For $Le = 1$ and $Le = 0.7$, we found that flames are non-symmetric for low values of the gas-solid heat transfer coefficient b in the considered fairly wide channels and become mushroom-shaped symmetric as b is increased, extinguishing for large values of b. This confirms that heat losses contribute to the stabilization of symmetric flames, at least for these values of Le close to unity. The acoustic oscillations are more important for non-symmetric

flames in long channels (here for $L = 2400\delta_T$) and for symmetric flames in the case of shorter channels ($L = 800\delta_T$).

For $Le = 0.3$, flames appear to be non-symmetric for all the studied values of b, breaking into small round-shaped cells as the heat transfer coefficient b becomes large. These cellular flames present large burning rates and are therefore robust to heat losses. As a consequence, they do not extinguish as b is increased within the considered range, and can propagate to the channel end. Moreover, all the studied $Le = 0.3$ flames present large pressure oscillations. This $Le = 0.3$ case is relevant for lean hydrogen flames, and the present results show two important features to be taken into account in the design of lean hydrogen burners: the robustness of lean hydrogen flames to heat losses, that can be related to the formation of cellular round-shaped fast-burning flames and the onset of large amplitude flame-acoustic oscillations that can affect the stability and even the integrity of the system.

This paper is also a reminder that attention should be given to the possible symmetry breaking in computations of flames propagating in ducts. If, as it is frequently done, symmetry of the flame is assumed in simulations, the flame burning and propagation rate, and the possibility of occurrence of acoustic flame instabilities can be mispredicted.

6. Acknowledgments

This work is part of project #PID2019-108592RB-C42 funded by MCIN / AEI / 10.13039/ 501100011033.

The authors thankfully acknowledge the computer resources at MARENOSTRUM and CIBELES and technical support provided by Barcelona Super-

computing Center and UAM (projects RES-FI-2019-1-0042, IM-2019-2-0006, IM-2020-1-0009 and IM-2020-2-0027).

AppendixA. Fuel consumption rate property

For the sake of completeness, the expression for the fuel consumption rate is derived below. Let us consider an adiabatic channel. Using a reference frame attached to the flame front (for example, to a point with a given temperature) and writing the equation for the fuel mas fraction in a conservative form, we have:

$$\frac{\partial \rho Y}{\partial t} + \frac{\partial}{\partial x_i}\left\{\rho Y[u_i + \delta_{ix} u_f(t)] - \rho \mathcal{D}\frac{\partial Y}{\partial x_i}\right\} = -\dot{\omega}\,, \tag{A.1}$$

where $u_f(t)$ is the instantaneous reference frame speed.

Integrating Eq. A.1 over a sufficiently large volume of the channel enclosing the flame, one can obtain:

$$\int_{x_1}^{x_2}\int_{0}^{D} \frac{\partial \rho Y}{\partial t}\, dx\, dy - \rho_0 Y_0 u_f(t) D = -\int_{x_1}^{x_2}\int_{0}^{D} \dot{\omega}\, dx\, dy\,. \tag{A.2}$$

where points x_1 and x_2 are chosen far ahead and far behind the flame. In writing Eq. A.2, it was also used that

$$x = x_1: \quad u_i \to 0, \quad Y \to Y_0; \quad \text{and} \quad x = x_2: \quad Y \to 0. \tag{A.3}$$

When the flame is moving steadily ($\partial/\partial t \equiv 0$), the first term in Eq. A.2 is exactly zero and $S_c \equiv u_f$. When the flame is far from the ends of the channel, it is convenient to replace the integration limits with $x_1 = 0$ and $x_2 = L$, since $\dot{\omega}$ is vanishingly small far from the flame.

In the general case, we can still use

$$S_c = \frac{1}{\rho_0 Y_0 D} \int_0^L \int_0^D \dot{\omega}\, dx\, dy \tag{A.4}$$

to characterize the flame dynamics. This coincides with the flame speed relative to the walls when the flame moves at a constant velocity and is close to the value of the front propagation velocity in the time dependent case. However, it is obvious from its derivation that S_c can significantly differ from the actual flame speed, u_f, in very short channels (say, $L \sim O(\delta_T)$) or when the flame is situated close to the left (closed) or right (open) ends of the channel. For this reason, the use of S_c in these cases is not appropriate and, possibly, may lead to erroneous conclusions.

References

[1] C. Jiménez, D. Fernández-Galisteo, V. Kurdyumov, Flame-acoustics interaction for symmetric and non-symmetric flames propagating in a narrow duct from an open to a closed end, Combust. Flame 225 (2021) 499–512.

[2] W. Kaskan, An investigation of vibrating flames, 4th Symposium on Combustion 4 (1953) 575–591.

[3] G. Searby, Acoustic instability in premixed flames, Combust. Sci. Technol. 81 (1992) 221–231.

[4] R. Aldredge, N. Killingsworth, Experimental evaluation of Markstein number influence on thermoacoustic instability, Combust. Flame 137 (2004) 178–197.

[5] J. Yáñez, M. Kuznetsov, Flame instabilities of lean hydrogen-air mixtures in a smooth open-ended vertical channel, Combust. Flame 162 (2013) 2830–2839.

[6] F. Veiga-López, D. Martínez-Ruiz, E. Fernández-Tarrazo, M. Sánchez-Sanz, Experimental analysis of oscillatory premixed flames in a Hele-Shaw cell propagating towards a closed end, Combust. Flame 201 (2019) 1–11.

[7] F. Veiga-López, D. Martínez-Ruiz, M. Kuznetsov, M. Sánchez-Sanz, Thermoacoustic analysis of lean premixed hydrogen flames in narrow vertical channels, Fuel 278 (2020) 118212.

[8] E. Flores-Montoya, V. Muntean, M. Sánchez-Sanz, D. Martínez-Ruiz, Non-adiabatic modulation of premixed-flame thermoacoustic frequencies in slender tubes, J. Fluid Mech. 933 (2022) A50.

[9] A. Dubey, Y. Koyama, N. Hashimoto, P. Fujita, Acoustic parametric instability, its suppression and a beating instability in a mesoscale combustion tube, Combust. Flame 228 (2021) 277–291.

[10] C. H. Tsai, The asymmetric behavior of steady laminar flame propagation in ducts, Combust. Sci. Technol. 180 (2008) 533–545.

[11] V. N. Kurdyumov, Lewis number effect on the propagation of premixed flames in narrow adiabatic channels: Symmetric and non-symmetric flames and their linear stability analysis, Combust. Flame 158 (2011) 1307–1317.

[12] V. Kurdyumov, C. Jiménez, Propagation of symmetric and non-symmetric premixed flames in narrow channels: influence of conductive heat-losses, Combust. Flame 161 (2014) 927–936.

[13] M. Sánchez-Sanz, D. Fernández-Galisteo, V. Kurdyumov, Effect of the equivalence ratio, Damköhler number, Lewis number and heat release on the stability of laminar premixed flames in microchannels, Combust. Flame 161 (2014) 1282–1293.

[14] D. Fernández-Galisteo, C. Jiménez, M. Sánchez-Sanz, V. Kurdyumov, The differential diffusion effect of the intermediate species on the stability of premixed flames propagating in microchannels, Combust. Theory Model. 18 (2014) 582–605.

[15] C. Jiménez, D. Fernández-Galisteo, V. Kurdyumov, DNS study of the propagation and flashback conditions of lean hydrogen-air flames in narrow channels: Symmetric and non-symmetric solutions, Int. J. Hydrogen Energy 40 (2015) 12541–12549.

[16] C. Jiménez, V. Kurdyumov, Propagation of symmetric and non-symmetric lean hydrogen-air flames in narrow channels: Influence of heat losses., Proc. Combust. Inst. 36 (2017) 1559–1567.

[17] K. Bioche, A. Pieyre, G. Riber, F. Richecoeur, L. Vervisch, The role of gravity in the asymmetry of flames in narrow combustion chambers, Combust. Flame 203 (2019) 238–246.

[18] A. Dejoan, V. Kurdyumov, Thermal expansion effect on the propagation of premixed flames in narrow channels of circular cross-section: Multi-

plicity of solutions, axisymmetry and non-axisymmetry, Proc. Combust. Inst. 37 (2019) 1927–1935.

[19] A. Dejoan, C. Jiménez, V. Kurdyumov, Critical conditions for non-symmetric flame propagation in narrow channels: influence of the flow rate, the thermal expansion, the Lewis number and heat-losses, Combust. Flame 209 (2019) 430–440.

[20] K. Bhairapurada, B. Denet, P. Boivin, A lattice-boltzmann study of premixed flames thermo-acoustic instabilities, Combust. Flame 240 (2022) 112049.

[21] A. Petchenko, V. Bychkov, V. Akkerman, L. Eriksson, Violent folding of a flame front in a flame-acoustic resonance, Phys. Rev. Lett. 97 (2006) 164501.

[22] A. Petchenko, V. Bychkov, V. Akkerman, L. Eriksson, Flame-sound interaction in tubes with nonslip walls, Combust. Flame 149 (2007) 418–434.

[23] G. Searby, D. Rochwerger, A parametric-acoustic instability in premixed flames, J. Fluid Mech. 231 (1991) 529–543.

[24] P. Pelcé, D. Rochwerger, Vibratory instability of cellular flames propagating in tubes, J. Fluid Mech. 239 (1992) 293–307.

[25] F. Higuera, Acoustic response of a lean premixed flame propagating upward in a tube, Combust. Flame 199 (2019) 377–386.

[26] T. Poinsot, S. Lele, Boundary conditions for direct simulations of compressible reacting flows, J. Comp. Physics 101 (1992) 104–129.

[27] T. Poinsot, D. Veynante, Theoretical and Numerical Combustion, 3d. edition, available at www.cerfacs.fr/elearning ed., 2012.

[28] A. Ghani, T. Poinsot, L. Gicquel, G.Staffelbach, LES of longitudinal and transverse self-excited combustion instabilities in a bluff-body stabilized turbulent premixed flame, Combust. Flame 162 (2015) 4075–4083.

[29] T. Kaiser, G. Öztarlik, L. Selle, T. Poinsot, Impact of symmetry breaking on the flame transfer function of a laminar premixed flame, Proc. Combust. Inst. 37 (2019) 1953–1960.

[30] T. Schuller, T. Poinsot, S. Candel, Dynamics and control of premixed combustion systems based on flame transfer and describing functions, J. Fluid Mech. 894 (2020) P1.

[31] T. Poinsot, D. Veynante, S. Candel, Quenching processes and premixed turbulent combustion diagrams, J. Fluid Mech. 228 (1991) 561606.

[32] H. Schmidt, C. Jiménez, Numerical study of the direct pressure effect of acoustic waves in planar premixed flames, Combust. Flame 157 (2010) 1610–1619.

[33] C. Jiménez, J. Quinard, J. Graña-Otero, H. Schmidt, G. Searby, Unsteady response of hydrogen and methane flames to pressure waves, Combust. Flame 159 (2012) 1894–.1908.

[34] J. Grcar, A new type of steady and stable, laminar, premixed flame in ultra-lean, hydrogen-air combustion, Proc. Combust. Inst. 32 (2009) 1011–1018.

[35] D. Martínez-Ruiz, F. Veiga-López, D. Fernández-Galisteo, V. Kurdyumov, M. Sánchez-Sanz, The role of conductive heat losses on the formation of isolated flame cells in Hele-Shaw chambers, Combust. Flame 209 (2019) 187199.